TEXAS A&M UNIVERSITY
College Station, Texas

HYBRID METHODS FOR

ROTORDYNAMIC ANALYSIS

(NASA-CR-17[illegible]) [illegible] [illegible]
[illegible] ANALYSIS [illegible] (Univ.)
[illegible] p [illegible] CSCL 13K
[illegible]

prepared for

George C. Marshall

Space Flight Center

Alabama 35812

under

CONTRACT NAS8 - 36182

Principal Investigator

Sherif T. Noah

Mechanical Engineering Department

Texas A&M University

College Station, Texas 77843

December 1986

TABLE OF CONTENTS

ABSTRACT

Effective procedures are presented for the response analysis of the SSME turbopumps under transient loading conditions. Of particular concern is the determination of the nonlinear response of the systems to rotor imbalance in presence of bearing clearances. The proposed procedures take advantage of the nonlinearities involved being localized at only few rotor/housing coupling points.

The methods include those based on integral formulations for the incremental solutions involving the transition matrices of the rotor and housing. Alternatively, a convolutional representation of the housing displacements at the coupling points is proposed which would allow performing the transient analysis on a reduced model of the housing. The integral approach is applied to small dynamical models to demonstrate the efficiency of the approach

For purposes of assessing the numerical integration results for the nonlinear rotor/housing systems, a numerical harmonic balance procedure is developed to enable determining all possible harmonic, subharmonic and nonperiodic solutions of the systems. A brief account of the Fourier approach is presented as applied to a two degree of freedom rotor-support system.

LIST OF FIGURES

LIST OF TABLES

I. INTRODUCTION

The dynamic transient response analysis of the SSME turbopumps is essential for further development and prediction of the engine performance under various load levels and required maneuvers. Childs [1] conducted numerical analysis for critical speed-transitions of the HPOTP. A rubbing condition was predicted for that earlier configuration at the turbine floating-ring seals during shutdown. More recently, Childs [2] concluded a series of studies concerning the development of a reliable RPL engine and a description of new problems which are being encountered in developing FPL performance. The analysis was based on a modal method developed earlier by the same author [3]. Childs [2] demonstrated that although a linear transient analysis remains an efficient procedure for general characterization of the turbopump's rotor-dynamics, nonlinear analysis is essential. An important case considered by Childs is that of the effect of the radial clearances provided at the outer races of the bearings. The results of the nonlinear analysis showed a significant reduction in the subsynchronous rotor motion. More significantly, the bearing clearances can drop the peak-vibration running speed into the operating range where the synchronous whirling loads might pose a serious threat to bearing life.

For large complex rotor systems, such as the SSME turbopumps, various modeling and analysis techniques vary in their ability to accurately describe the systems' behavior. This ability mainly

depends on the configuration of the systems analyzed and on the forcing conditions. In rotating components, this also involves whether the rotating speed is constant or varying with time. A hybrid representation by various types of coordinates and formulation for the various components of the systems may prove valuable.

Different procedures have been utilized by analysts to determine the transient response of large order rotor systems. The procedures can be recognized as falling under one of two basic approaches. Those using physical or modal coordinates of the complete system and those using the coordinates of the individual components of the system. The methods also differ in the numerical integration methods selected for the analysis.

Rouch and Kao [4] employed Guyan (static) reduction method to arrive at a reduced size model in terms of the remaining physical coordinates. Accuracy of the results could be expected to be acceptable since the rotor is basically a train of mass-stiffness subsystems. Nordmann [5] attempted to minimize the inaccuracy of static condensation by applying the static reduction technique to an arbitrarily substructured rotor system and then assemble the reduced substructures to form a reduced system. The procedures is very laborious and no guarantees of accuracy are apparent.

Childs [6] utilized free-interface modes of the various system components to represent the assembled SSME turbopumps. The method, using fourth order Runge-Kutta integration, does not provide for accommodating accurate modal representation of the large housing model while maintaining a small size for the model. Nelson et al. [7] on

the other hand used fixed-interface complex component modes to assemble a reduced size model. For systems with large number of coupling points among the components, the approach suffers the problem of introducing higher frequencies resulting from excessive number of constraints imposed at the coupling (or boundary) points. In a transient analysis, this will necessarily result in much smaller time increments and consequently, will lead to excessive computational time and larger round-off errors.

For nonlinear large rotor systems, only a few analysts have presented techniques for the general transient analysis of such systems. Adams [8] used a normal mode representation for the rotor in terms of its undamped, free symmetric modes and treated gyroscopic and nonlinear terms as pseudo-external loads. The method presented by Childs [6] makes use of a similar procedure to couple the rotor to its flexible housing. Nelson et al. [7] developed a general computer code for the transient analysis of large rotor systems. The user may utilize time-step integration in the constrained-rotor (fixed-interface) modal space. Again, all connection points, including those at the nonlinearities must be constrained, leading to the same shortcomings described previously.

None of the above studies have adequately addressed the problems of attempting to use reduced size, accurate models and the associated efficiency of computation. A judicious selection of the system configurations and the numerical methods is essential for achieving the required efficiency while maintaining acceptable accuracy.

In this study, integration methods based on the transition matrices [9] of the separate rotor and housing are used to efficiently determine the nonlinear transient coupled system response under imbalance forces and in presence of bearing clearances. Pragenau [10] utilized the transition matrix for integration, stating that it offers the simplicity of the Euler method without requiring small steps. Pragenau maintained that for constant subsystems, the stability and accuracy of the method are acquired through the closed form solution of the transition matrix.

Alternatively, a discretized Duhamel [9] (convolution) integral method can be used to an advantage to represent the response at the housing coupling points to the rotor. Kubomura [11] used a convolution based method to achieve dynamic condensation of a substructure to its coupling points to other structures. Convolution was also used in [12,13] to reduce system coordinates to that of the nonlinearities.

Along with the response analysis in presence of bearing clearances under imbalance forces, a numerical harmonic balance method is developed toward verifying possible steady state synchronous and subsynchronous rotor response. This is essential to ensure that no possible potentially damaging solution is missed due to unfortunate selections of particular initial conditions. The harmonic method locates all possible periodic solutions. The method is briefly presented here from references [14] and [15] as applied to a modified Jeffcott model.

II. THE TURBOPUMP MODEL

Housing:

The modal equations of the housing in the X-Z, Y-Z planes in terms of a truncated set of its modal coordinates $\{q_H\}$, normalized with respect to the mass matrix, can be written as [16,17]

$$\{\ddot{q}_H\} + [2\,\xi_H\,\Lambda_H^{\frac{1}{2}}]\,\{\dot{q}_H\} + [\Lambda_H]\,\{q_H\} = [A_{HC}]^T\,\{F_H\} \qquad (1)$$

where ξ_H and Λ_H are the modal damping coefficients and natural frequencies, respectively, F_H is the vector of coupling forces to the rotor, including the balance piston axial force. The axial force is a function of the axial displacement and velocity as well as the spinning speed. The coupled physical displacements in the X and Y directions at the coupling points to the rotor are given by

$$\{W_H\} = \begin{Bmatrix} X \\ Y \end{Bmatrix} = [A_{HC}]\,\{q_H\} \qquad (2)$$

where $[A_{HC}]$ is the normalized modal vectors, with respect to the mass matrix, associated with the coupling points.

Rotor:

As in the case of housing, the symmetric-rotor equations of motion may be written in terms of a truncated set of modal coordinates $\{q_R\}$ of the free-free nonspinning, undamped rotor as

$$\{\ddot{q}_R\} + [D_R]\,\{\dot{q}_R\} + [\Gamma_R]\,\{q_R\} = [A_{RC}]^T\{F'_R + P'_R\} \qquad (3)$$

where D_R and Γ_R are nondiagonal matrices which are speed, $\dot{\psi}$, dependent, and P'_R is the imbalance forces which is, in general, functions of $\dot{\psi}$ and $\ddot{\psi}$. The vector F'_R represents the interaction forces with the housing such as the bearing, seal, side loads (which are functions of $\dot{\psi}$), etc. the physical displacements at these coupling points are given by

$$\{W_R\} = \begin{Bmatrix} X_R \\ Y_R \end{Bmatrix} = \begin{bmatrix} A'^T_{RC} & 0_T \\ 0 & A'^T_{RC} \end{bmatrix} \{q_R\} = [A^T_{RC}] \{q_R\} \tag{4}$$

Interaction Forces

The coupling forces between the housing and rotor can be expressed as (see Fig. 1) [17]

$$-\{F_H\} = [C] \{\mathring{W}_H\} + [K] \{W_H\} - [C] \{\mathring{W}_R\} - [K] \{W_R\} \tag{5}$$

and

$$\{F_R\} = \{F_H\} \tag{6}$$

where [C] and [K] involve direct and cross coupled stiffness and damping forces as well as spinning velocity dependent coefficients. The coefficients of the bearing forces allow for presence of clearances (deadbands).

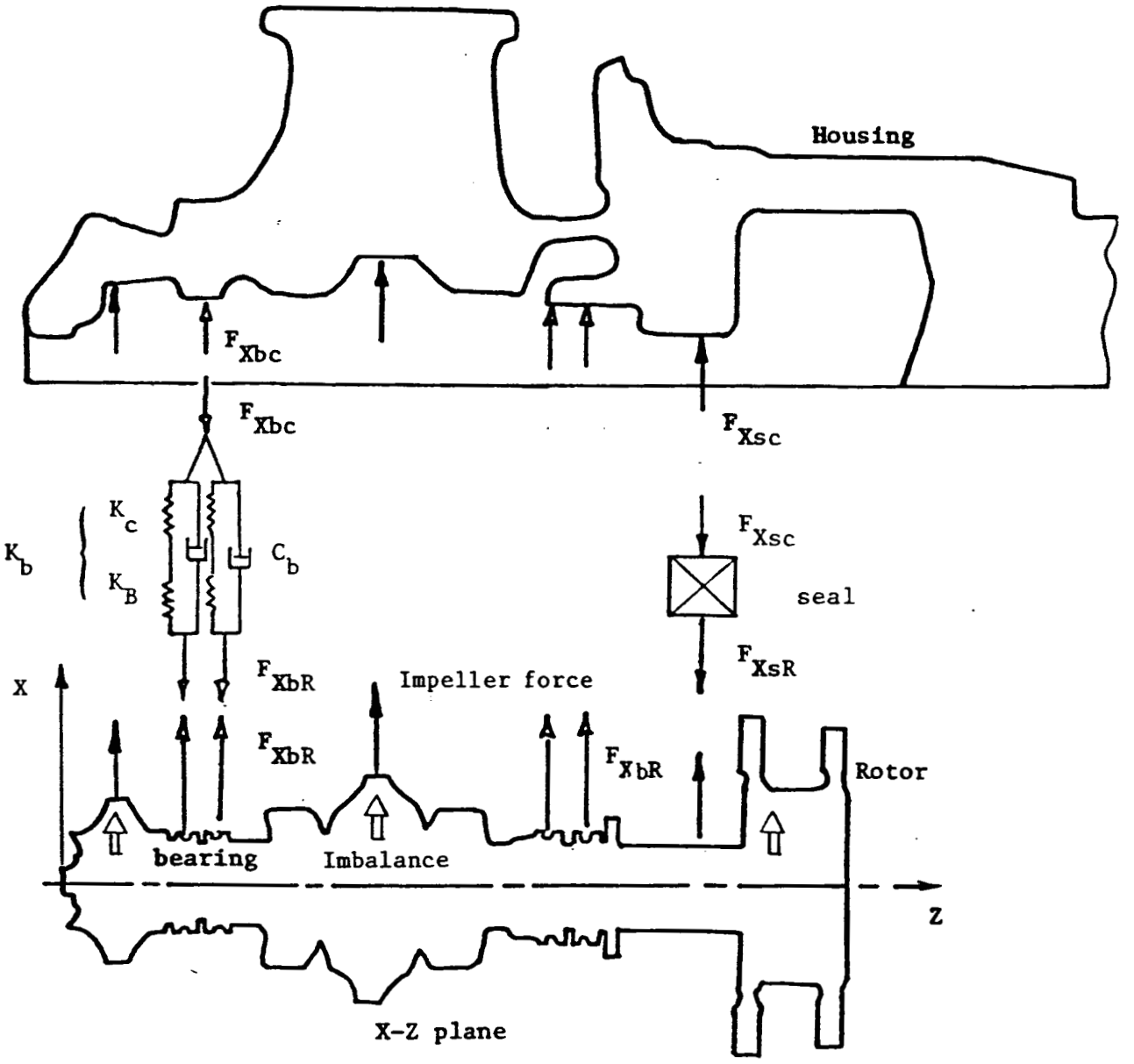

Figure 1. Coupling elements and forces in the HPOTP.

III. TRANSITION MATRIX FORMULATIONS

The rotor's modal equations of motion are written in the first order form

$$\{\dot{U}_R\} = [\alpha_R]\ \{U_R\} + \{F_R\} \tag{7}$$

where

$$\{U_R\} = \begin{Bmatrix} q_R \\ \dot{q}_R \end{Bmatrix}\ ,\quad [\alpha_R] = \begin{bmatrix} 0 & I \\ -\Gamma_R & -D_R \end{bmatrix} \tag{8}$$

and

$$\{F_R\} = \{A_{RC}{}^T\{F_R' + P_R'\}\} \tag{9}$$

Similar first order equations can be written for the housing.

The solution of equations (7) with constant rotating speed and the analogous ones for the housing in terms of the associated transition matrices of the rotor and housing takes the form [9]

$$\{U(t)\} = e^{[\alpha]t}\ \{U(0)\} + \int_0^t e^{[\alpha](t-\tau)}\{F(\tau)\}\ d\tau \tag{10}$$

This representation can be cast in discretized form as

$$\{U_{i+1}\} = e^{[\alpha]T}\{U_i\} + \int_{t_i}^{t_{i+1}} e^{[\alpha](t_{i+1}-t)}\ \{F(t)\}\ dt \tag{11}$$

where $\{U_i\} \equiv \{U(t_i)\}$

and $$T = t_{i+1} - t_i \tag{12}$$

The force vector in eq. (11) can be either treated as (i) constant within a small time increment T or (ii) a linear function of time. Clearly, the linear representation would result in more accuracy for a given increment T. An assumption of a step load (constant load within an increment) allows equation (11) to be written in the simple form

$$\{U_{i+1}\} = [\Phi(T)]\ \{U_i\} + ([\Phi(T)] - [\text{`I}_\text{.}]\ [\alpha]^{-1}\ \{F_i\} \tag{13}$$

where $$[\Phi(T)] = e^{[\alpha]T}\ ,\quad \{F_i\} = \{F(t_i)\} \tag{14}$$

$$e^{[\alpha]T} = \sum_{n=0}^{\infty} \frac{T^n}{n!}\ [\alpha]^n \tag{15}$$

so that $$(\Phi(T) - I)\ [\alpha]^{-1} = T\left[[\text{`I}_\text{.}] + \sum_{n=1}^{\infty} \frac{T^n}{(n+1)!}\ [\alpha]^n\right] \tag{16}$$

Both expressions in (15) and (16) converge very rapidly for small increment, T, and when used as above (constant [α]), need only be calculated once for the entire time response history of the coupled rotor/housing system.

A more efficient algorithm can be constructed by representing the coupling forces as linear functions of time within each increment T, or

$$\{F(t)\} = \{F_i\} + \frac{t - t_i}{T}\ (\{F_{i+1}\} - \{F_i\}) \tag{17}$$

Using this representation, and after some manipulation, the solution (11) can be shown to take the form [10]

$$\{U_{i+1}\} = [\Phi]\{U_i\} + \left[[\Phi] - [I]\right][\alpha]^{-1}\left(\{F_i\} + [\alpha]^{-1}\frac{\{F_{i+1}\}-\{F_i\}}{T}\right) - [\alpha]^{-1}\left(\{F_{i+1}\} - \{F_i\}\right) \quad (18)$$

An incremental solution using equation (18) for the rotor and a similar matrix equation for the housing, along with equations (5) and (6) in first order form, can be employed to construct the response time history of the turbopump considered. The particular recurrence procedure used will depend on the type of transient response sought as well as on the accuracy versus computational time tradeoffs. Some discussion of the computational procedure is presented in a later section.

Use of The Duhamel Integral

An efficient incremental representation of the housing displacements can be achieved using the convolution integral. As with the transition matrix formulation, the coupling forces are treated as external loads on the housing and may be assumed linear in time for every increment T. The response at any time t is given for zero initial conditions, using equation (1), as

$$\{W_H\} = [A_{HC}]\int_o^t \left[\frac{1}{\omega_d} e^{-\xi_n\omega_n(t-\tau)} \sin\omega_d(t-\tau)\right][A_{HC}]^{tr}\{F_H(\tau)\}d\tau \quad (19)$$

or

$$\{W_H(t)\} = \sum_{j=1}^{N}\{A_{HC}\}^{(j)}\{A_{HC}^{tr}\}^{(j)}\int_o^t \frac{e^{-\xi_n\omega_n(t-\tau)}}{\omega_j} \sin\omega_j(t-\tau)\{F(\tau)\}\,d\tau \quad (20)$$

Where $\{A_{HC}\}^{(j)}$ is a reduced column matrix of elements of the jth eigenvector associated with the coupling points of the housing and rotor, ω_d is the damped natural frequency of the nth mode and "tr" stands for a transpose.

To enhance the accuracy of the modal representation of the housing, the deleted higher housing modes can be approximately accounted for through the residual flexibility corresponding to these modes, or at any time t,

$$\{W_H\} = [A_{HC}]\ \{q_H\} + [G_H]\ \{F_H\} \quad , \tag{21}$$

where $[G_H]$ is the residual flexibility matrix corresponding to the coupling points on the housing's nth mode of the uncoupled housing.

For the purpose of demonstrating the method in simpler terms, consider the generalized housing coordinate of the undamped nth mode

$$q_n(t) = \frac{1}{\omega_n} \int_o^t \sin \omega_n(t-\tau)\ P_n(\tau)\ d\tau \tag{22}$$

where $P_n(\tau)$ is the unknown modal coupling force. If the force is assumed linear in time within each increment, the generalized displacement in equation (22) due to a coupling force applied between t_i and t_{i+1} is given by

$$q_n(t) = \frac{1}{\omega_n} \int_{t_i}^{t_{i+1}} \left\{P_n(t_i) + \frac{\tau - t_i}{T}\left(P_n(t_{i+1}) - P_n(t_i)\right)\right\} \sin \omega_n(t-\tau) d\tau \tag{23}$$

After some manipulation, the integration in equation (23) can be written in closed form in terms of the unknowns P_n's as

$$q_n(t) = \frac{1}{\omega_n^2}\{\cos \omega_n t \left[P_n(t_{i+1}) \cos \omega_n t_{i+1} - P_n(t_i) \cos \omega_n t_i - \frac{P_n(t_{i+1}) - P_n(t_i)}{\omega_n} (\sin \omega_n t_{i+1} - \sin \omega_n t_i)\right] + \sin \omega_n t \left[P_n(t_{i+1}) \sin \omega_n t_{i+1} - P_n(t_i) \sin \omega_n t_i + \frac{P_n(t_{i+1}) - P_n(t_i)}{\omega_n} (\cos \omega_n t_{i+1} - \cos \omega_n t_i)\right]\} \quad (24)$$

or $$q_n(t) = \frac{1}{\omega_n^2}\{A^{(i)} \cos \omega_n t + B^{(i)} \sin \omega_n t\} \quad (25)$$

The total response at time t due to the contribution of the coupling forces from zero to time t (= N.T.) is

$$q_n(t) = \frac{1}{\omega_n^2}\left[\cos \omega_n NT \sum_{i=0}^{N} A_i^{(i)} + \sin \omega_n NT \sum_{i=0}^{N} B_i^{(i)}\right] \quad (26)$$

The generalized velocity can be expressed as

$$\dot{q}_n(t) = \frac{1}{\omega_n}\left[\cos \omega_n N.T \sum_{i=0}^{N} B^{(i)} - \sin \omega_n N.T \sum_{i=0}^{N} A^{(i)}\right] \quad (27)$$

The generalized acceleration can be obtained from

$$\ddot{q}_n(t) = -\omega_n^2 q_n(t) + P_n(t) \quad (28)$$

The generalized displacements and velocities of the rotor in incremental form are given previously in the form of equation (18). Equations

(18), (27), (5) and (6) can be readily employed to calculate the response time history for the coupled rotor/housing system.

Computational Procedures and Results

Various alternative procedures have been explored for the efficient implementation of the integral formulations based on the transition matrices and the convolution integral. Although studies are continuing to fully make use of the computational advantages offered by these formulations, the following appears to be the most attractive to date.

For both the transition and convolution methods, a linearized representation of the coupling forces (including those at the bearing deadband) are utilized. Equations of the form of (18), (26) and (27) are used along with the coupling forces relations given by (5) and (6). If the rotor system is linear, the forces are expressed in terms of the displacements at the coupling points. The system is then represented by a simultaneous system of equations involving the housing and rotor coupling coordinates so that at each increment of time

$$\{W_{t_{i+1}}\} = \{f(W_{t_i}, F_{t_i})\} \tag{29}$$

where f stands for a function.

Another alternative which proves to be very effective specially in presence of the bearing deadband nonlinearity is by again using a lineared force variation within each time increment, but including an iterative procedure at each time step. The iteration work as follows,

where F stands for coupling forces: Predict the response at the coupling points at t_{i+1} from those at t_i

$$W'_{H_{i+1}} = f_H (W_{H_i}, W_{R_i}, F_{H_i})$$
$$W'_{R_{i+1}} = f_R (W_{H_i}, W_{R_i}, F_{R_i}, \text{imbalance forces}) \tag{30}$$

Then predict the forces at t_{i+1} from

$$F'_{H_{i+1}} = f'_H (W'_{H_{i+1}}, W'_{R_{i+1}})$$
$$F'_{R_{i+1}} = f'_R (W'_{H_{i+1}}, W'_{R_{i+1}}, \text{imbalance forces}) \tag{31}$$

Correct the displacements at t_{i+1} as

$$W_{H_{i+1}} = f_H (W_{H_i}, F_{H_i}, F'_{H_{i+1}})$$
$$W_{R_{i+1}} = f_R (W_{R_i}, F_{R_i}, F'_{R_{i+1}}, \text{imbalance forces}) \tag{32}$$

Re-iterate using equations (31) and (32). If the maximum difference between the displacements in two consecutive iterations is smaller than a specified tolerance, the iteration is stopped and the final values of displacements at t_{i+1} are taken as

$$W'_{H_{i+1}} = W_{H_{i+1}}$$
$$W'_{R_{i+1}} = W_{R_{i+1}} \tag{33}$$

The transition matrix method was applied to a system consisting of damped two subsystems of three and two degrees of freedom interacting through a clearance. The results are presented in the Appendix, in which comparisons to the results obtained using an iterative Runge-Kutta method are made. The results show the transition matrix method

to be more efficient than that of the numerical integration procedure for a given time increment. However, more work is needed to devise an alternative iterative technique which would expand the range of convergence of the method.

For a subsystem to which the form of the convolution integral (19) is applicable, a solution procedure similar to that involving equations (30) to (33) can be applied using equation (26).

Alternatively, a one step procedure can be utilized if the coupling forces are assumed to be constant, rather than varying linearly, within each time step. In that case, the expression for $q_n(t)$ is obtained by setting

$$P_n(t_{i+1}) = P_n(t_i) = P_n$$

The efficiency of this formulation can be greatly enhanced by utilizing a Taylor series expansion for the displacements at time t_{i+1} in terms of the displacements and their derivatives at t_i, or

$$W_{t_{i+1}} = W_{t_i} + \overset{\circ}{W}_{t_i} (t_{i+1} - t_i) + \frac{1}{2} \overset{\circ\circ}{W}_{t_i} (t_{i+1} - t_i)^2 \qquad (34)$$

where $\overset{\circ}{W}_{ti}$ and $\overset{\circ\circ}{W}_{ti}$ are given by appropriate expressions of the forms given by equations (27) and (28). The displacements (and velocities) as in equation (34) are used to calculate the coupling force in each time step.

An approach combining the Duhamel representation for the housing of a rotor system and a transition matrix algorithm for the rotor

could be utilized to an advantage in determining the transient response of the system. The approach is yet to be applied to rotor-housing systems.

IV. NUMERICAL HARMONIC BALANCE METHOD

A method is developed [15] in order to check all possible nonlinear responses of simple rotor systems under periodic imbalance loads in presence of bearing clearances, rubbing, seal forces, side forces and others. The method requires the spinning speed of the rotor to be constant so that the model is represented by a nonhomogeneous system of nonlinear equations of constant coefficients. The developed method is a modification of that due to Yamauchi [18].

The early work in nonlinear rotordynamics by Yamamoto [20] introduces a nonlinearity to the Jeffcott equation by including the effect of bearing clearances. The Van der Pol self-sustained vibration theory was used for the analysis under the assumption of small clearances. Due to the symmetry of the gaps, only the harmonic response was considered. Recently, Childs [21] presented an explanation for the subharmonic response of rotors in presence of bearing clearances and a side load, using perturbation techniques under the assumption of small nonlinearity. The potential destructive vibration of the LOX pump in presence of rub in the SSME (Space Shuttle Main Engine) has been considered by Beatty [22].

Glease and Bukley [23] used a direct numerical integration method to analyze the rotor response, including seal and nonlinear bearing forces. However, the results only show the transient response before a steady-state is reached. Since the damping is usually small in rotor systems, a steady-state response is often established after a relatively long period of integration time. For the steady-state

response, Yamauchi [18] developed a numerical harmonic balance method using the FFT (Fast Fourier Transformation) algorithm for nonlinear multiple degrees of freedom rotor systems, in which transfer matrix formulations were used to describe the system. Saito [19] calculated the nonlinear unbalance response of horizontal Jeffcott rotors. Both studies of Yamauchi and Saito were concerned only with the harmonic response. No analysis for the important case of subharmonic rotor response was attempted.

The procedure developed in [15], and presented here, is based on a modified numerical harmonic balance method using discrete Fourier transformation and its inverse. This transformation, rather than an FFT procedure, was utilized in order to reduce computational time and errors. This is achieved by calculating the complex exponential values at the beginning of computation and then store them in active memory for subsequent calculations. Subharmonic and superharmonic responses are also accounted for by the method. An account of the method and some results obtained for the response of the modified Jeffcott rotor system selected for the analysis is outlined in what follows.

The Modified Jeffcott Model

The rotor model is depicted in Fig. 2. In the figure, ω is the shaft speed which is assumed constant, and ψ is the angle of the disk rotation with respect to the inertial coordinate system y - z and is referred to as the whirl angle. The displacement of the rotor center from the origin of the inertial references frame is denoted by $\vec{r}$. The

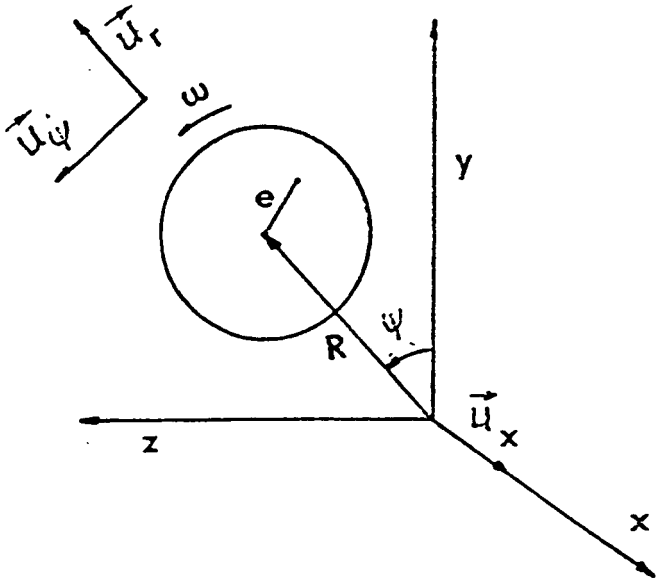

Figure 2. Coordinate system of rotor.

eccentricity, e, denotes the displacement of the mass center from the geometric center of the shaft.

The forces considered in the formulation of the equation of motion include bearing forces, seal forces, an imbalance force and a side force. The bearing forces can be assumed as piecewise-linear and occur only when the displacement of the shaft is greater than the clearance (or deadband) between bearing outer race and support. Friction due to rubbing between shaft and bearing support during contacts is also considered. The bearing forces, F_b, can be expressed as follows.

$$\vec{F}_b = \begin{cases} K_b(\vec{r}-\delta\vec{u}_r) + \mu K_b u_x \, X \, (\vec{r}-\delta\vec{u}_r) & ; \quad |r| \geq \delta \\ 0 & ; \quad |r| < \delta \end{cases} \tag{35}$$

in which $\vec{u}_r$ and $\vec{u}_x$ are unit vectors in the r and x direction, respectively, K_b is the bearing stiffness, δ is the deadband and μ is the coefficient of friction between shaft and bearing. The "X" stands for a vector cross product. The assumed form representing the seal forces is given by

$$\vec{F}_s = -C_s\dot{\vec{r}} - K_s\vec{r} + Q_s u_x \, X \, \vec{r} \tag{36}$$

Where K_s is the seal direct stiffness, C_s is the seal damping coefficient, and Q_s is the seal cross-coupling stiffness. The side force is assumed to be due to gravity. The gravity loading provides a side force in the negative direction.

The force equilibrium equations for the rotor can be written, with respect to the y - z inertia reference coordinates, as follows:

$$M\ddot{y} + C_s\dot{y} + K_s y + Q_s z + K_b\left|\left(y - y\frac{\delta}{\sqrt{y^2 + z^2}}\right)\right|$$

$$- \mu K_b\left|\left(z - z\frac{\delta}{\sqrt{y^2 + z^2}}\right)\right| = Me\omega^2 \cos\omega t - Mg \qquad (37\text{-a})$$

$$M\ddot{z} + C_s\dot{z} + K_s z - Q_s y + K_b\left|\left(z - z\frac{\delta}{\sqrt{y^2 + z^2}}\right)\right|$$

$$+ \mu K_b\left|\left(y - y\frac{\delta}{\sqrt{y^2 + z^2}}\right)\right| = Me\omega^2 \sin\omega t, \qquad (37\text{-b})$$

in which M is the mass of the disk, g is the acceleration of gravity, and $\left|\ \right|$ denotes that the nonlinear bearing forces occur only when $\sqrt{y^2 + z^2} >$; otherwise, they are zero. In the above equations, the rubbing between stator and blade tip instead of bearing rubbing (which is usually small) can be calculated by changing K_b to that of the stator stiffness.

The equations of motions, (37-a) and (37-b), can be put in nondimentionalized form using the deadband, δ, as the reference displacement and the natural frequency of the associated linear problems ($\delta = 0$) as the reference frequency. This natural frequency is not that of the nonlinear system, although due to small clearance the periods of maintained contact during rotation may lead to a frequency close to that of the associated linear frequency. Let

$$K_q = K_s + K_b \qquad \omega_n^2 = \frac{K_q}{M} \qquad \Omega = \frac{\omega}{\omega_n}$$

$$\alpha = \frac{K_s}{K_q} \qquad \beta = \frac{K_b}{K_q} \qquad \gamma = \frac{Q_s}{K_q} \qquad (38)$$

$$Y = \frac{y}{\delta} \qquad Z = \frac{z}{\delta} \qquad R = \sqrt{Y^2 + Z^2}$$

$$\varepsilon = \frac{e}{\delta} \qquad \zeta = \frac{C_s}{2M\omega_n} \qquad \phi = \frac{g}{\omega_n^2 \delta}$$

$$\nu\theta = \omega t$$

where θ is a normalized time, and ν is the subharmonic order. Using the parameters in equation (38) with equations (37-a) and (37-b) leads to

$$Y'' + \frac{2\zeta\nu}{\Omega} Y' + \frac{\alpha\nu^2}{\Omega^2} Y + \gamma \frac{\nu^2}{\Omega^2} Z + G(\theta) - \mu F(\theta) = \varepsilon\nu^2 \cos(\nu\theta) + \phi\frac{\nu^2}{\Omega^2} \qquad (39\text{-a})$$

$$Z'' + \frac{2\zeta\nu}{\Omega} Z' + \frac{\alpha\nu^2}{\Omega^2} Z - \gamma \frac{\nu^2}{\Omega^2} Y + F(\theta) + \mu G(\theta) = \varepsilon\nu^2 \sin(\nu\theta) \qquad (39\text{-b})$$

where

$$G(\theta) = \beta\frac{\nu^2}{\Omega^2} Y \left| (1 - \frac{1}{R}) \right| \qquad (39\text{-c})$$

$$F(\theta) = \beta\frac{\nu^2}{\Omega^2} Z \left| (1 - \frac{1}{R}) \right| \qquad (39\text{-d})$$

in which a prime denotes differentiation with respect to the normalized time θ and the nonlinear restoring forces are established whenever R is greater than unity.

Method of Analysis

The steady periodic solution of equations (39), including any subharmonic, superharmonic or harmonic vibration can be written as Fourier series, or

$$Y(\theta) = a_{y0} + 2 \sum_{n=1}^{N} (a_{yn} \cos n\theta - b_{yn} \sin n\theta) \qquad (40\text{-a})$$

$$Z(\theta) = a_{z0} + 2 \sum_{n=1}^{N} (a_{zn} \cos n\theta - b_{zn} \sin n\theta) \qquad (40\text{-b})$$

where N is the number of harmonics to be taken into account in the final solution under the assumption of small frequency bandwidth. The multiple of two and the minus sign associated with the b_n are adopted to facilitate accommodating complex Fourier coefficients when discrete time data is used. In the same say, the time series representation of the nonlinear bearing forces, occurring only when $|R| > 1$, can be expressed as Fourier series of the form:

$$G(\theta) = c_{y0} + 2 \sum_{n=1}^{N} (c_{yn} \cos n\theta - d_{yn} \sin n\theta) \qquad (41\text{-b})$$

$$F(\theta) = c_{z0} + 2 \sum_{n=1}^{N} (c_{zn} \cos n\theta - d_{zn} \sin n\theta) \qquad (41\text{-b})$$

Since these nonlinear bearing forces are a consequence of the existence of a deadband in the system, the Fourier coefficients of the nonlinear restoring forces are functions of the Fourier coefficients of the steady periodic solution sought. Substituting equations (40) and (41) into equations (39-a) and (39-b) and applying a harmonic balance procedure yields 4N + 2 nonlinear simultaneous equations involving 8N + 4 unknowns. The harmonic balance procedure gives for the constant term:

$$\frac{\alpha\nu^2}{\Omega^2} a_{y0} + c_{y0} + \gamma \frac{\nu^2}{\Omega^2} a_{zo} - \mu c_{z0} = \phi\frac{\nu^2}{\Omega^2} \tag{42-a}$$

$$\frac{\alpha\nu^2}{\Omega^2} a_{z0} + c_{z0} - \gamma \frac{\nu^2}{\Omega^2} a_{yo} + \mu c_{y0} = 0 \tag{42-b}$$

the cosine terms:

$$-n^2 a_{yn} - n \frac{2\zeta\nu}{\Omega} b_{yn} + \alpha\frac{\nu^2}{\Omega^2} a_{yn} + c_{yn} + \gamma\frac{\nu^2}{\Omega^2} a_{zn} - \mu c_{zn} = 0.5m\varepsilon\nu^2 \tag{42-c}$$

$$-n^2 a_{zn} - n \frac{2\zeta\nu}{\Omega} b_{zn} + \alpha\frac{\nu^2}{\Omega^2} a_{zn} + c_{zn} - \gamma\frac{\nu^2}{\Omega^2} a_{yn} + \mu c_{yn} = 0 \tag{42-d}$$

and the sine terms:

$$n^2 b_{yn} - n \frac{2\zeta\nu}{\Omega} a_{yn} - \alpha\frac{\nu^2}{\Omega^2} b_{yn} - d_{yn} - \gamma\frac{\nu^2}{\Omega^2} b_{zn} + \mu d_{zn} = 0 \tag{42-e}$$

$$n^2 b_{zn} - n \frac{2\zeta\nu}{\Omega} a_{zn} - \alpha\frac{\nu^2}{\Omega^2} b_{zn} - d_{zn} + \gamma\frac{\nu^2}{\Omega^2} b_{yn} - \mu d_{yn} = 0.5m\varepsilon\nu^2 \tag{42-f}$$

in which

$$m = 0 \quad ; \quad n \neq \nu$$

$$m = 1 \quad ; \quad n = \nu$$

Another set of 4N + 2 equations can be found from the relationships between the Fourier coefficients of the nonlinear bearing forces and those of the steady-state periodic solution. These relationships can be found by determining $Y(\theta)$ and $Z(\theta)$ from the Fourier coefficients of the steady-state periodic solution using the discrete inverse Fourier transformation,

$$d_r = \text{Real}\left(\sum_{k=0}^{N-1} D_k e^{i(2\Pi kr/N)}\right) \tag{43}$$

where D_k stands for the Fourier coefficient, and d_r, for discrete displacement. Using equations (35), discrete time series of the nonlinear bearing force can be found. The inverse discrete Fourier transformation of the time series solution for the nonlinear bearing forces will yield the Fourier coefficients of the nonlinear bearing force as

$$D_k = \left(\sum_{r=0}^{N-1} d_r i(-2\Pi kr/N)\right) \tag{44}$$

The resulting nonlinear simultaneous algebraic equations can be handled using a Newton-Raphson method. The Newton-Raphson method uses an incremental procedure in determining the values for the next iteration as follows. Let

$$S = S^0 + \Delta S, \tag{45}$$

where S represents the Fourier coefficients of the steady-state solution, and the superscript "0" denotes current state while ΔS stands for the increments of the coefficients during one step of iteration. For example,

$$a_{yn} = a_{yn}^0 + \Delta a_{yn}$$

Similarly, the Fourier coefficients of the nonlinear restoring force can also be expressed as follows:

$$B + B^0 + \Delta B, \tag{46}$$

For example,

$$c_{yn} = c^{0}_{yn} + \Delta c_{yn}$$

in which the increment ΔB can be expressed using the total derivatives with respect to all the Fourier coefficients of the steady-state solution, S^0, so that

$$\Delta B = \sum_{n=1}^{4N+2} \frac{\partial B^0}{\partial S_n} \Delta S_n \qquad (47)$$

For example,

$$\Delta c_{yn} = \sum_{n=0}^{N} \left(\frac{\partial c_{yn}}{\partial a_{yn}} \Delta a_{yn} + \frac{\partial c_{yn}}{\partial a_{zn}} \Delta a_{zn}\right) + \sum_{n=1}^{N} \left(\frac{\partial c_{yn}}{\partial b_{yn}} \Delta b_{yn} + \frac{\partial c_{yn}}{\partial b_{zn}} \Delta b_{zn}\right)$$

where the partial derivatives are to be calculated at the current state value.

In order to account for the large nonlinearity in the system, the increments, ΔS_n, must be chosen small as compared to S_n whenever numerical differentiation is performed. The numerical differentiation is performed using forward differentiation. For example, to obtain the derivative $\frac{\partial c_{yn}}{\partial a_{yn}}$, a new c_{yn} is calculated at $a_{yn} = a^{0}_{yn} + \Delta a_{yn}$ from the nonlinear relations of equations (39-c) and (39-d). The numerical differentiation is then given by

$$\frac{\partial c_{yn}}{\partial a_{yn}} = \frac{c_{yn} - c^{0}_{yn}}{\Delta a_{yn}}$$

The numerical differentiation procedure can be done using forward differentiation as follows:

1. a_0 is changed by adding the preset small Δa_0, but other Fourier coefficients, a_n and b_n, are not changed.
2. The newly assumed discrete displacements, $Y(\theta)$ and $Z(\theta)$, are generated using a discrete inverse Fourier transform.
3. Discrete nonlinear forces, $G(\theta)$ and $F(\theta)$, are calculated using equations (39).
4. The Fourier coefficients of the discrete nonlinear force, c_0, c_n, and d_n, are calculated using Discrete Fourier Transformation.
5. The differential values of $\frac{\partial c_0}{\partial a_0}$, $\frac{\partial c_i}{\partial a_0}$, and $\frac{\partial d_i}{\partial a_0}$ are calculated
6. The calculations in step 1 to 5 are repeated for each a_i and b_i.

Substituting equations (45) and (46) into equations (42), the following incremental form will result,

$$\frac{\alpha\nu^2}{\Omega^2}\Delta a_{y0} + \Delta c_{y0} + \gamma\frac{\nu^2}{\Omega^2}\Delta a_{zo} - \mu\Delta c_{z0}$$

$$= \phi\frac{\nu^2}{\Omega^2} - \frac{\alpha\nu^2}{\Omega^2}a^0_{y0} - c^0_{y0} - \gamma\frac{\nu^2}{\Omega^2}a^0_{zo} + \mu c^0_{z0} \qquad (48\text{-a})$$

$$\frac{\alpha\nu^2}{\Omega^2}\Delta a_{z0} + \Delta c_{z0} - \gamma\frac{\nu^2}{\Omega^2}\Delta a_{yo} + \mu\Delta c_{y0}$$

$$= -\frac{\alpha\nu^2}{\Omega^2}a^0_{z0} - c^0_{z0} + \gamma\frac{\nu^2}{\Omega^2}a^0_{yo} - \mu c^0_{y0}, \qquad (48\text{-b})$$

for the cosine terms:

$$- n^2\Delta a_{yn} - n\frac{2\zeta\nu}{\Omega}\Delta b_{yn} + \alpha\frac{\nu^2}{\Omega^2}\Delta a_{yn} + \Delta c_{yn} + \gamma\frac{\nu^2}{\Omega^2}\Delta a_{zn} - \mu\Delta c_{zn}$$

$$= 0.5\, m\varepsilon\nu^2 + n^2 a^0_{yn} + n\frac{2\zeta\nu}{\Omega} b^0_{yn} - \alpha\frac{\nu^2}{\Omega^2} a^0_{yn} - c_{yn} - \gamma\frac{\nu^2}{\Omega^2} a^0_{zn} + \mu c^0_{zn} \quad (48\text{-c})$$

$$- n^2\Delta a_{zn} - n\frac{2\zeta\nu}{\Omega}\Delta b_{zn} + \alpha\frac{\nu^2}{\Omega^2}\Delta a_{zn} + \Delta c_{zn} - \gamma\frac{\nu^2}{\Omega^2}\Delta a_{yn} + \mu\Delta c_{yn}$$

$$= n^2 a^0_{zn} + n\frac{2\zeta\nu}{\Omega} b^0_{zn} - \alpha\frac{\nu^2}{\Omega^2} a^0_{zn} - c^0_{zn} + \gamma\frac{\nu^2}{\Omega^2} a^0_{yn} - \mu c^0_{yn} \quad (48\text{-d})$$

and for the sine terms:

$$n^2\Delta b_{yn} - n\frac{2\zeta\nu}{\Omega}\Delta a_{yn} - \alpha\frac{\nu^2}{\Omega^2}\Delta b_{yn} - \Delta d_{yn} - \gamma\frac{\nu^2}{\Omega^2}\Delta b_{zn} + \mu\Delta d_{zn}$$

$$= - n^2 b^0_{yn} + n\frac{2\zeta\nu}{\Omega} a^0_{yn} + \alpha\frac{\nu^2}{\Omega^2} b^0_{yn} + d^0_{yn} + \gamma\frac{\nu^2}{\Omega^2} b^0_{zn} - \mu d^0_{zn} \quad (48\text{-e})$$

$$n^2\Delta b_{zn} - n\frac{2\zeta\nu}{\Omega}\Delta a_{zn} - \alpha\frac{\nu^2}{\Omega^2}\Delta b_{zn} - \Delta d_{zn} + \gamma\frac{\nu^2}{\Omega^2}\Delta b_{yn} - \mu\Delta d_{yn}$$

$$= 0.5\, m\varepsilon\nu^2 - n^2 b^0_{zn} + n\frac{2\zeta\nu}{\Omega} a^0_{zn} + \alpha\frac{\nu^2}{\Omega^2} b^0_{zn} + d^0_{zn} - \gamma\frac{\nu^2}{\Omega^2} b^0_{yn} + \mu d^0_{yn} \quad (48\text{-f})$$

in which

$$m = 0 \quad ; \quad n \neq \nu$$

$$m = 1 \quad ; \quad n = \nu$$

Equations (48-a) to (48-f) can be put in the matrix form

$$[K]\{\Delta_X\} = \{W\} \quad (49)$$

Where [K] corresponds to the Jacobian matrix whose elements are evaluated at every step.

This iteration is continued until all the components of the correction vector {W} become sufficiently close to zero. The calculation procedure presented here is basically an iterative procedure. By setting the initial values to zero, a linear solution is calculated in the first iteration. The linear solution is modified as the iteration progresses. For the next frequency ratio, the final solution of the previous step frequency ratio is used to facilitate the convergence of the iteration.

Numerical Results and Discussion

A comparison between results using direct numerical integration and those of the FFT method is shown in Fig. 3. The numerical integration is carried out using the central difference method with the nondimensional equations (39-a) and (39-b). To find the steady-state solution within a reasonable duration, the damping factor, ζ, is chosen to be relatively large. For the application of the FFT method in a numerical procedure, four harmonic coefficients are taken into account for each of the displacements, Y and Z. Also, sixteen discrete data points are chosen in one period to avoid the aliasing effects. The mean displacements, $\bar{Y}$, $\bar{Z}$, and $\bar{R}$, are defined as half of the sum of the maximum displacement and the minimum displacement in a steady-state response. As shown in Fig. 3, the frequency response results using the FFT method demonstrate good agreement with those of the direct numerical integration method.

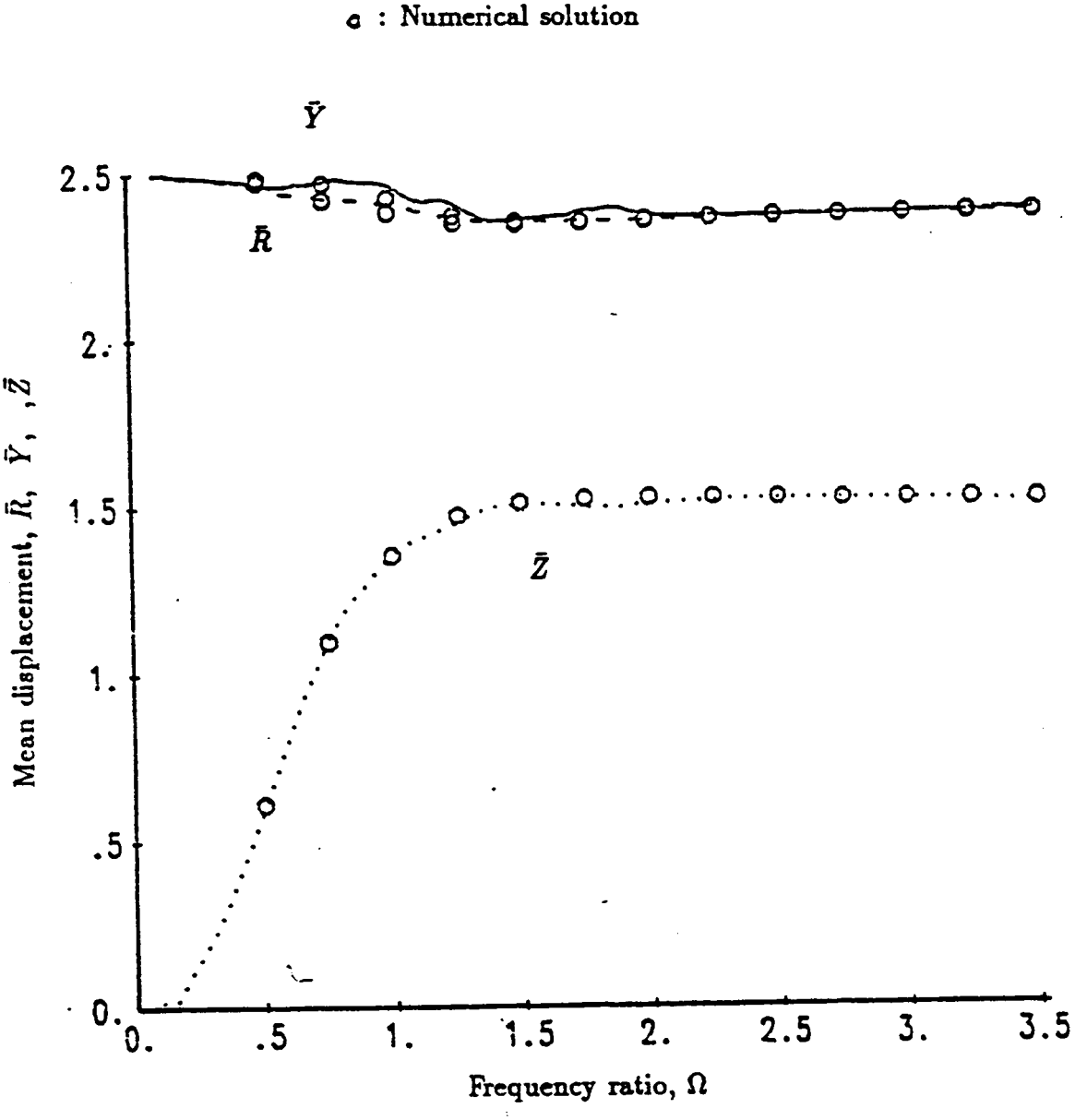

Figure 3. Comparison between numerical and FFT solutions;
$\alpha = 0.01$, $\beta = 1.$, $\gamma = 0$, $\zeta = 0.5$, $\varepsilon = 1.5$, $\phi = 1.5$, $\mu = 0$

In Fig. 4, the nonlinear response of the system is shown in presence of the side force due to gravity. To ensure the occurrence of subharmonic response, the damping factor, ζ, was set to zero. As depicted in Fig. 4, a second-order superharmonic resonance occurs near the frequency ratio of 0.5. A second-order subharmonic resonance occurs below the frequency ratio of two, while a third-subharmonic resonance appears below the frequency ratio of three. These trends have already been demonstrated experimentally by Bently [26] and Erich [27]. The nonlinear steady-state analysis also reveals the co-existence of harmonic response with the subharmonic response. The occurrence of a specific type of response depends upon the particular initial conditions (due to proximity to a corresponding domain of attraction).

A comparison between the nonlinear response and harmonic motions in the y-z plane can be made by examining the results presented in Fig. 5, 6, and 7. The shaft center traces noncrossing paths in a harmonic response case, or otherwise the paths will be of more complicated shapes and larger radii (a less desirable behavior in rotating machinery). The existence of second-order subharmonic resonances is examined for various values of the nondimensionalized side force factor, $\phi = \frac{g}{\omega_n^2 \delta}$, in Fig. 8. The figure shows that subharmonic vibration would not exist for either zero or relatively large values of ϕ. This is because only symmetric motion is maintained for these particular values of ϕ. Fig. 8 also shows that a smaller ϕ value results in a subharmonic response within a broader frequency range. The choice of a smaller clearance or a softer bearing stiffness can, therefore,

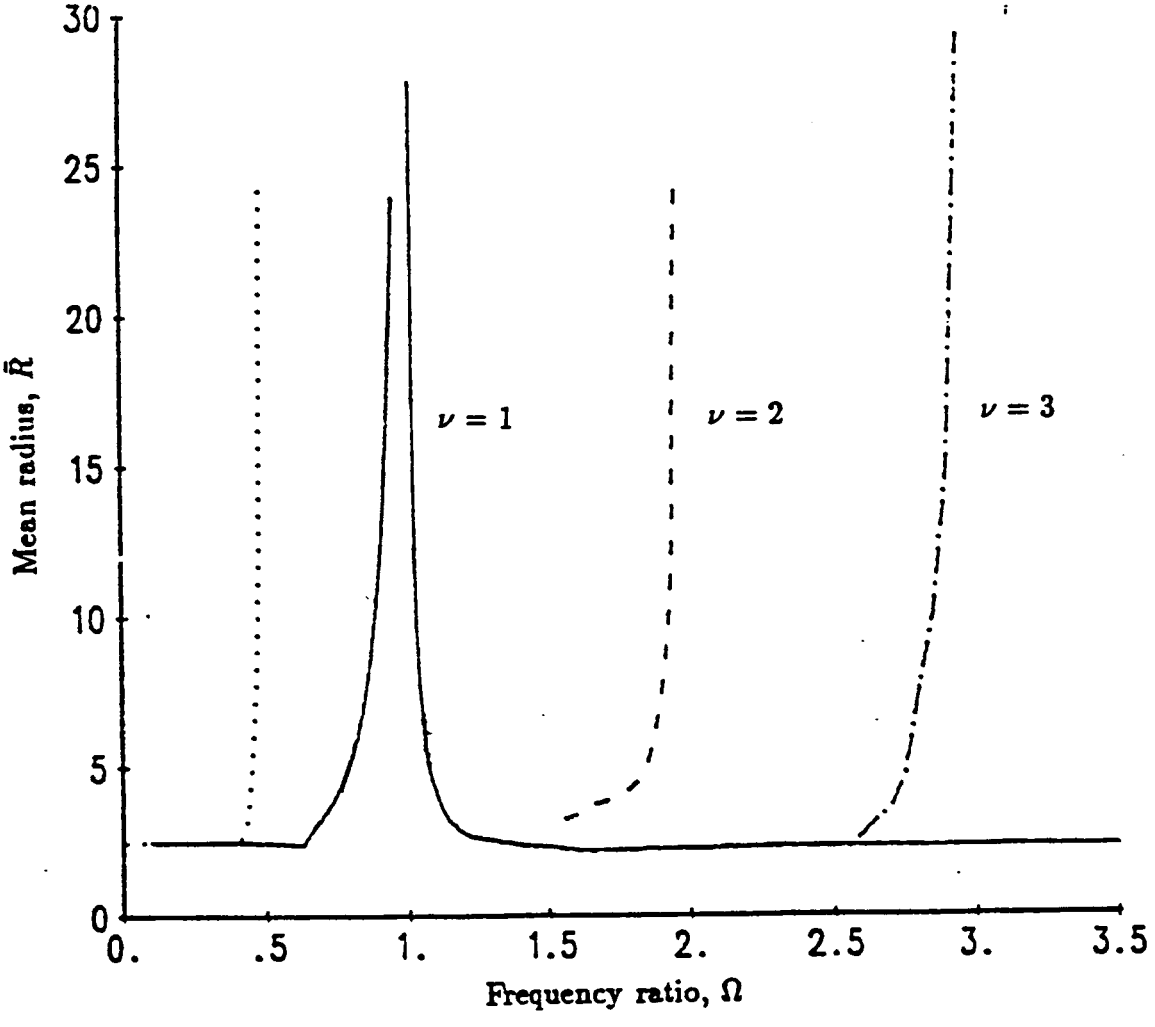

Figure 4. Superharmonic and subharmonic resonance in rotor dynamic response; $\alpha = 0.01$, $\beta = 1.$, $\gamma = 0$, $\zeta = 0$, $\varepsilon = 1.5$, $\phi = 1.5$, $\mu = 0.$

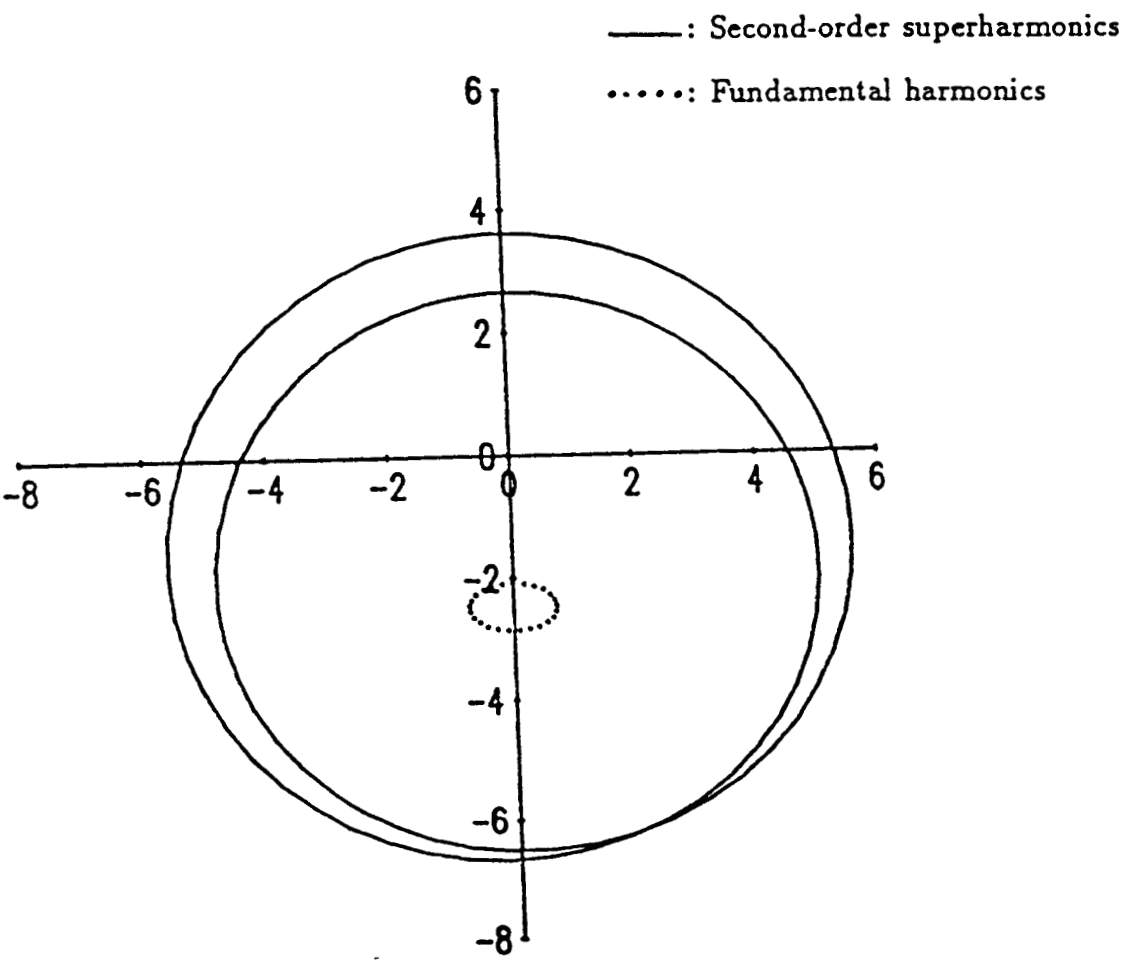

Figure 5. Superharmonic response at $\Omega = 0.45$;
$\alpha = 0.01$, $\beta = 1.$, $\gamma = 0$, $\zeta = 0$,
$\varepsilon = 1.5$, $\phi = 1.5$, $\mu = 0.$

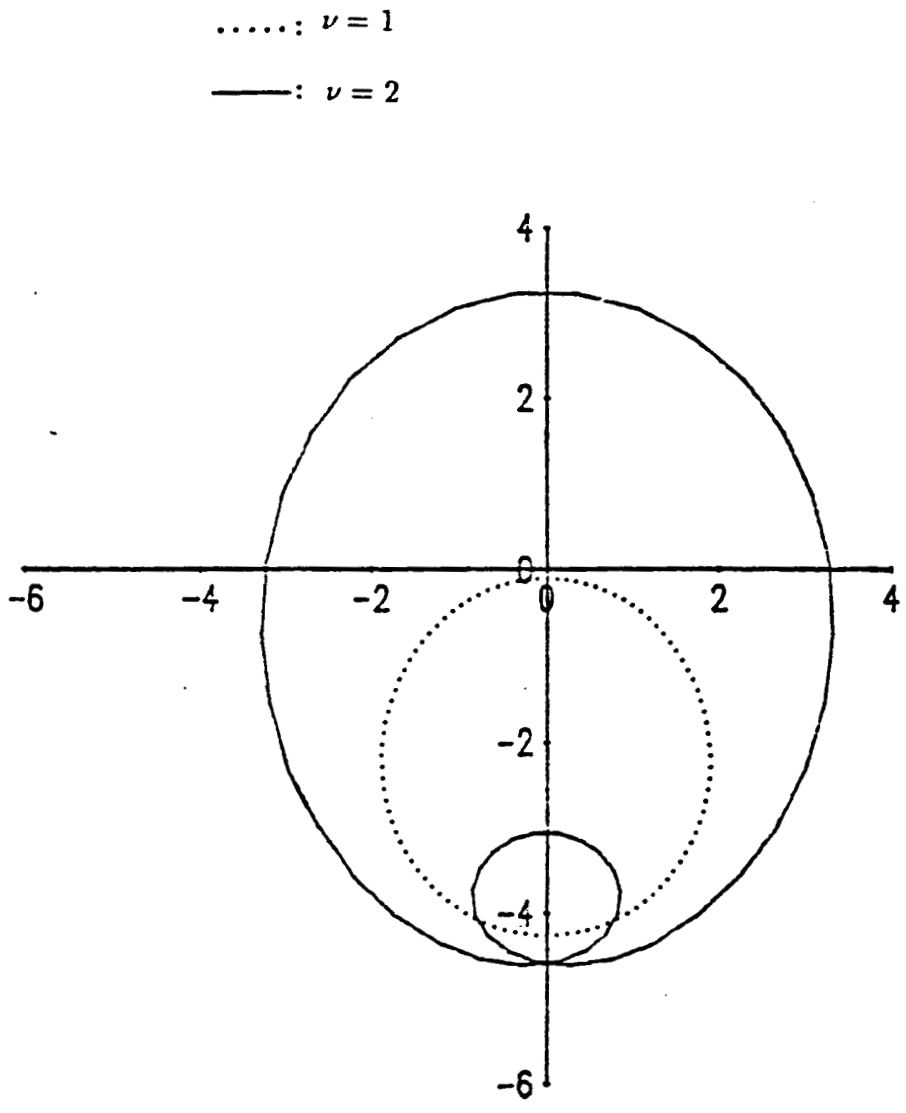

Figure 6. Second-order subharmonic response at $\Omega = 1.7$; $\alpha = 0.01$, $\beta = 1.$, $\gamma = 0$, $\zeta = 0$, $\varepsilon = 1.5$, $\phi = 1.5$, $\mu = 0$

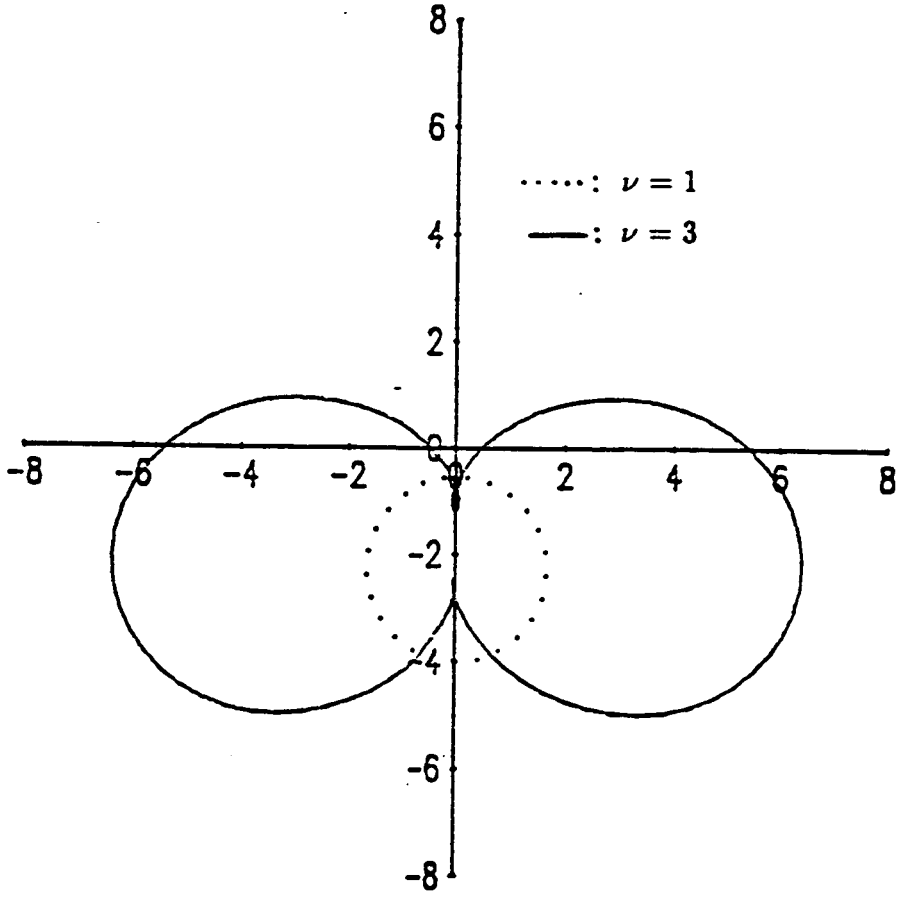

Figure 7. Third-order subharmonic response at $\Omega = 2.7$; $\alpha = 0.01$, $\beta = 1.$, $\gamma = 0$, $\zeta = 0$, $\varepsilon = 1.5$, $\phi = 1.5$, $\mu = 0.$

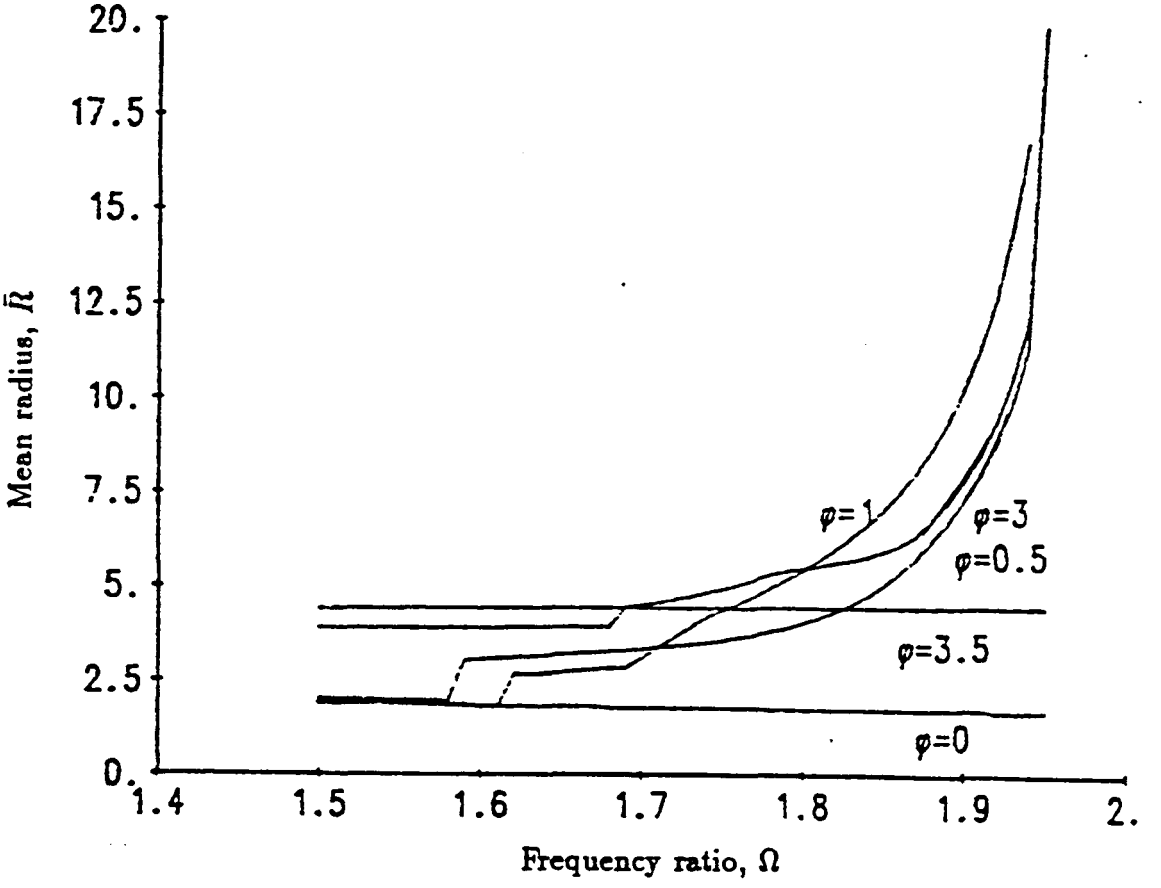

Figure 8. Effect of side force on nonlinear rotor dynamic response; $\alpha = 0.01$, $\beta = 1.$, $\gamma = 0$, $\zeta = 0.1$, $\varepsilon = 1.5$, $\mu = 0.$

reduce the possibility of a damaging resonance. The effect of eccentricity can be deduced from the examination of Fig. 9. A larger eccentricity influences the horizontal motion (z-direction) more than it does the vertical motion.

Other results concerning the effect of rubbing due to friction, damping, and cross-coupling stiffness can be found in reference [15].

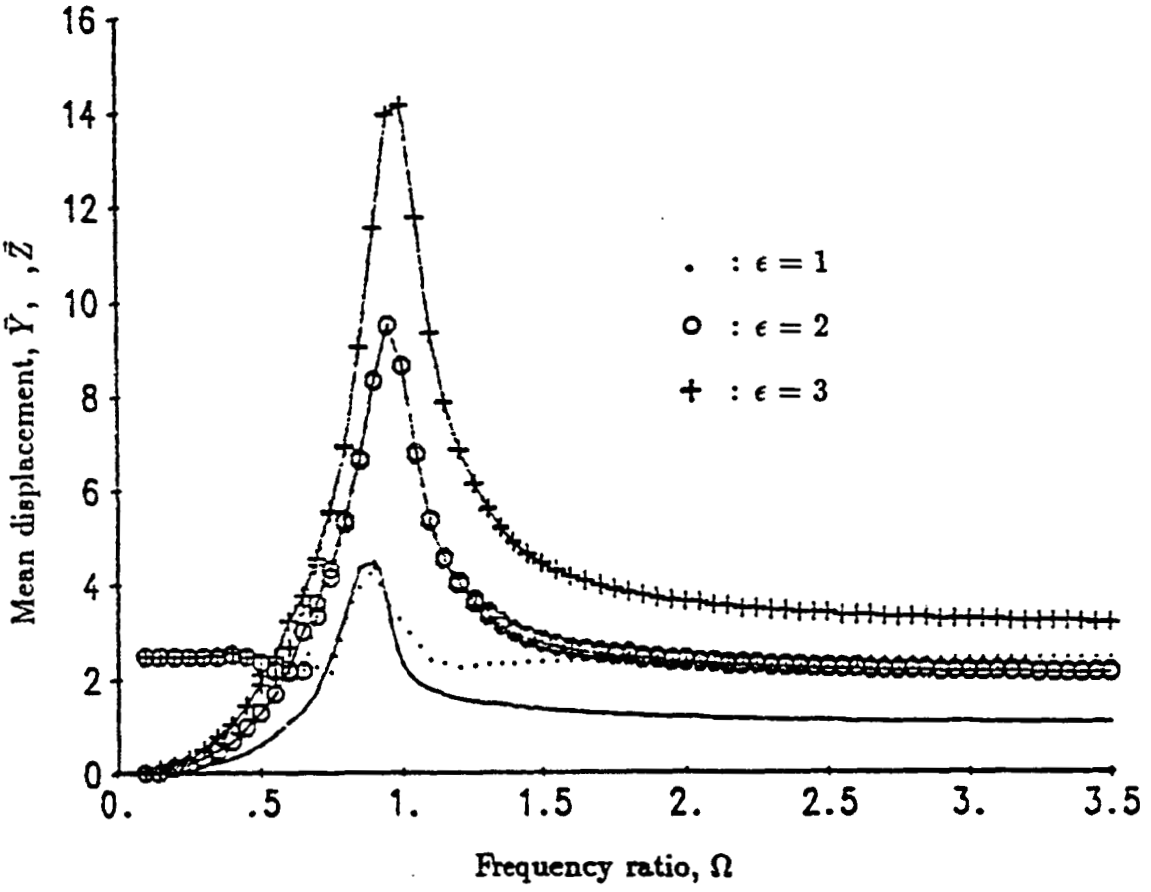

Figure 9. Effect of eccentricity on nonlinear rotor dynamic response; $\alpha = 0.01$, $\beta = 1.$, $\gamma = 0$, $\zeta = 0.1$, $\phi = 1.5$, $\mu = 0$ . . . . . .

V. USE OF COMPONENT MODE METHODS

A modified fixed interface component mode procedure of Glasgow and Nelson [24] can be applied to certain nonlinear rotor systems with flexible housing. The nonlinearity is assumed to arise from the existence of clearances at the bearings. The coupling between a rotor and its housing occurs through bearing, seal, fluid and other interaction forces.

The modified analysis procedure can be carried out as follows. The rotor and housing are coupled at their points of interaction except at the bearings with deadband clearances. The eigen-parameters of the coupled system are obtained with the rotor and housing fixed at the locations of the deadbands. The coupled system is then represented by a truncated set of these modes plus a static constrained mode [24] corresponding to the degrees of freedom at the location of the bearing clearances.

The fixed-interface component method was applied to two simple multi-degree of freedom subsystems and the results showed it to be more accurate than the original Nelson's method for the same total combined number of dynamic and static modes of the system. This is so since the method as modified above allows including more numbers of dynamic coordinates of the components in the analysis. The modified method becomes more efficient than the original method in cases where interaction forces occur at relatively large numbers of locations between the rotor and housing. The modified approach would allow first coupling the housing and rotor using more numbers of modes than

currently being used, then reduce the number of modes of the resulting coupled system.

VI. DISCUSSION AND RECOMMENDATIONS

1. Hybrid component representation and numerical incremental procedures for the transient response analysis of complex rotor systems can lead to more efficient methods.
2. The explicit integration methods based on the transition matrices and convolution can be very effective in determining the transient response of large flexible rotor/housing systems such as the SSME turbopumps. The methods are particularly efficient in cases concerning constant spinning rotor speeds and in presence of bearing deadband clearances. More work is, however, still needed to exploit and further develop the methods to their fullest potential.
3. A modified fixed-interference component mode method could be used to construct a reduced size rotor/housing system which is more accurate than that of the original method of reference [24]. The modification concerns the use of smaller number of connection points as the fixed interfaces of the system. Similarly, the hybrid coupling method of McNeal [25] could be extended for application to rotor systems.
4. A numerical harmonic balance method using discrete Fourier Transformation is developed and applied to a modified Jeffcott model including bearing clearances, seal cross coupling forces, a side force and friction due to rubbing. The method can be used to determine all possible steady state solutions for the rotor. The method can be extended to larger rotor systems, taking advantage

of the nonlinearities involved being localized. Application of the method will ensure that no potentially damaging periodic nonlinear response of a given rotor will be missed by solely depending on numerical integration methods. Arbitrarily selected initial conditions may not necessarily lead to a possible periodic solution using integration techniques. The determination of the domains of attraction with multiple solutions and the extension of the algorithm to multi-degree of freedom rotor systems are currently under consideration.

ACKNOWLEDGEMENT

The author is grateful to Thomas Fox of NASA, Marshall, for his input concerning the numerical harmonic balance method as to similar methods used in nonlinear control analysis and related studies. His frequent feedback to the author concerning the study and his enthusiastic support is appreciated. The author also appreciates the input and helpful comments offered by Dara Childs of Texas A&M University concerning some of the ideas used in this study.

REFERENCES

1. Childs, D. W., Transient Rotordynamic Analysis for the Space-Shuttle Main Engine High Pressure Oxygen Turbopump," J. Spacecraft, Vol. 12, No. 1 (1975), pp. 3-4.

2. Childs, D. W. and Moyer, D. S., "Vibration Characteristics of the HPOTP (High Pressure Oxygen Turbopump) of the SSME (Space Shuttle Main Engine), ASME Paper No. 84-GT-31, International Gas Turbine Conference, Amsterdam, Netherlands, June 1984.

3. Childs, D. W., "Two Jeffcott-Based Modal Simulation Models for Flexible Rotating Equipment," ASME J. Engineering for Industry, Vol. 97, No. 3 (1975), pp. 1000-1014.

4. Rouch, K. E. and Kao, J. S., "Dynamic Reduction in Rotor Dynamics by the Finite Element Method, ASME J. of Mechanical Design, Vol. 102, (1980) pp. 360-368.

5. Nordmann, R., "Eigenvalues and Resonance Frequency Forms of Turborotors with Sleeve Bearings Crank Excitation, External and Internal Damping," Machine Dynamics Group, Technical University Darmstadt, West Germany, June, 1975.

6. Childs, D. W., "The Space Shuttle Main Engine High-Pressure Fuel Turbopump-Rotordynamic Instability Problem," ASME J. Engineering for Power, Vol. 100, 1978, pp. 48-51.

7. Nelson, H. D., Meacham, W. L., Fleming, D. P. and Kascak, A. F., "Nonlinear Analysis of Rotor Bearing Systems Using Component Mode Synthesis," ASME Paper No. 82-GT-303, 1982.

8. Adams, M. L., "Non-Linear Dynamics of Flexible Multi-Bearing Rotors," J. Sound and Vibration, Vol. 71 (1980), pp. 129-144.

9. Meirovitch, L., Computational Methods in Structural Dynamics, Sijthoff and Noordhoff, 1980.

10. Von Pragenau, G. L., "Large Step Integration for Linear Dynamic Systems," Conference Proc. IEEE Southeastcon '81, reprint, April 1981.

11. Kubomura, K., "Transient Loads Analysis by Dynamic Condensation," ASME, J. Applied Mechanics, Vol. 52 (1985), pp. 559-564.

12. Tongue, B. H. and Dowell, E. H., "Component Mode Analysis of Nonlinear, Nonconservative Systems," ASME J. Appl. Mechanics, Vol. 50, 1983, pp. 204-209.

13. Clough, R. W. and Wilson, E. L., "Dynamic Analysis of Large Structural Systems with Local Nonlinearities," Computer Methods in Applied Mechanics and Engineering, Vol. 17/18 (1979), 107-129.

14. Choi, Y.-S. and Noah, S. T., "Forced Periodic Vibration of Unsymmetric Piecewise-Linear Systems," to be published in the J. of Sound and Vibration.

15. Choi, Y.-S. and Noah, S. T., "Nonlinear Steady-State Response of a Rotor-Support System," Submitted to the ASME J. of Vibration, Acoustics, Stress and Reliability in Design.

16. Childs, D. W., "Rotordynamic Analysis for the HPOTP of the SSME," Interim Progress Report for NASA Contract NAS8-31233, The University of Louisville/Speed Scientific School, Sept. 1979.

17. Noah, S. T., "Rotordynamic Analysis of the SSME Turbopumps Using Reduced Models," Final Report, NASA Contract NAS8-34505, Texas A&M University, Sept. 1984.

18. Yamauchi, S., "The Nonlinear Vibration of Flexible Rotors, 1st Report Development of a New Analysis Technique," Trans JSME, Vol. 49, No. 446, Series C Oct. 1983, pp. 1862-1868.

19. Saito, S., "Calculation of Nonlinear Unbalance Response of Horizontal Jeffcott Rotors Supported by Ball Bearings with Radial Clearances," ASME Paper No. 85-DET-33.

20. Yamamoto, T. T., "On Critical Speeds of a Shaft," Memoirs of the Faculty of Engineering, Nagoya (Japan) University, Vol. 6, No. 2, 1954.

21. Childs, D. W., "Fractional-Frequency Rotor Motion due to Nonsymmetric Clearance Effects," ASME, Journal of Energy and Power, Vol. 104, 1982, pp. 533-541.

22. Beatty, R. F., "Differentiating Rotor Response Due to Radial Rubbing," ASME, J. of Vibration, Acoustics, Stress, and Reliability in Design, Vol. 107, 1985, pp. 151-160.

23. Glease, J. R., and Bukley, P., "Effect of Bearing Deadbands on Bearing Loads and Rotor Stability," MSFC Advanced High Pressure O_2/H_2 Technology Conference Proceedings G. Marshall Space Flight Center; Huntsville, Alabama, June 27-29, 1984.

24. Glasgow, D. A., and Nelson, H. D., "Stability Analysis of Rotor-Bearing Systems Using Component Mode Synthesis," ASME J. of Mechanical Design, Vol. 102, No. 2, April 1980, pp. 352-359.

25. MacNeal, R. H., "A Hybrid Method of Component Mode Synthesis," Computers and Structures, Vol. 1, 1971, pp. 581-601.

26. Bently, D., "Forced Subrotative Speed Dynamic Action of Rotating Machinery," ASME paper No. 74-PET-16, Petroleum Mechanical Engineering Conference, Dallas, Texas, Sept. 1979.

27. Erich, F. F., "Subharmonic Vibrations of Rotors in Bearing Clearance," ASME paper No. 66-MD-1, Design Engineering Conference and Show, Chicago, Ill., May 9-12, 1966.

APPENDIX

The Transient Response of a Test Model

Two single mass spring subsystems interacting through a gap are utilized to form the test model (see Fig. A.1). Modal representation of the subsystems is utilized. The transient analysis is carried out using both the integral transition matrix method and an iterative Runge-Kutta-Verner integration scheme. A comparison of the computation time of both methods is shown in Table A.1. The comparison shows the transition matrix procedure to be more efficient.

TABLE A.1. Comparison of the Solution Time Calculated by Direct Integration and the Transition Matrix Methods

I. USING ALL THE SUBSYSTEMS MODES			
Time Step Size	Number of Steps	CPU Computation Time	
		Runge-Kutta-Verner	Transition Matrix
1×10^{-4}	45000	15 min. 26.7 sec.	4 min. 20.5 sec.
3×10^{-4}	15000	10 15	4 19.1
1×10^{-3}	4500	8 46.3	4 17.8
2×10^{-3}	2250	8 27	diverge
3×10^{-3}	1500	9 1.2	diverge
II. USING ONE MODE OF SUBSYSTEM B AND TWO MODES OF A			
1×10^{-4}	45000	8 min. 59.8 sec.	5 min. 22.4 sec.
3×10^{-4}	15000	3 16.6	2 35.9
1×10^{-3}	4500	3 2.8	1 43.6
2×10^{-3}	2250	3 12.3	diverge

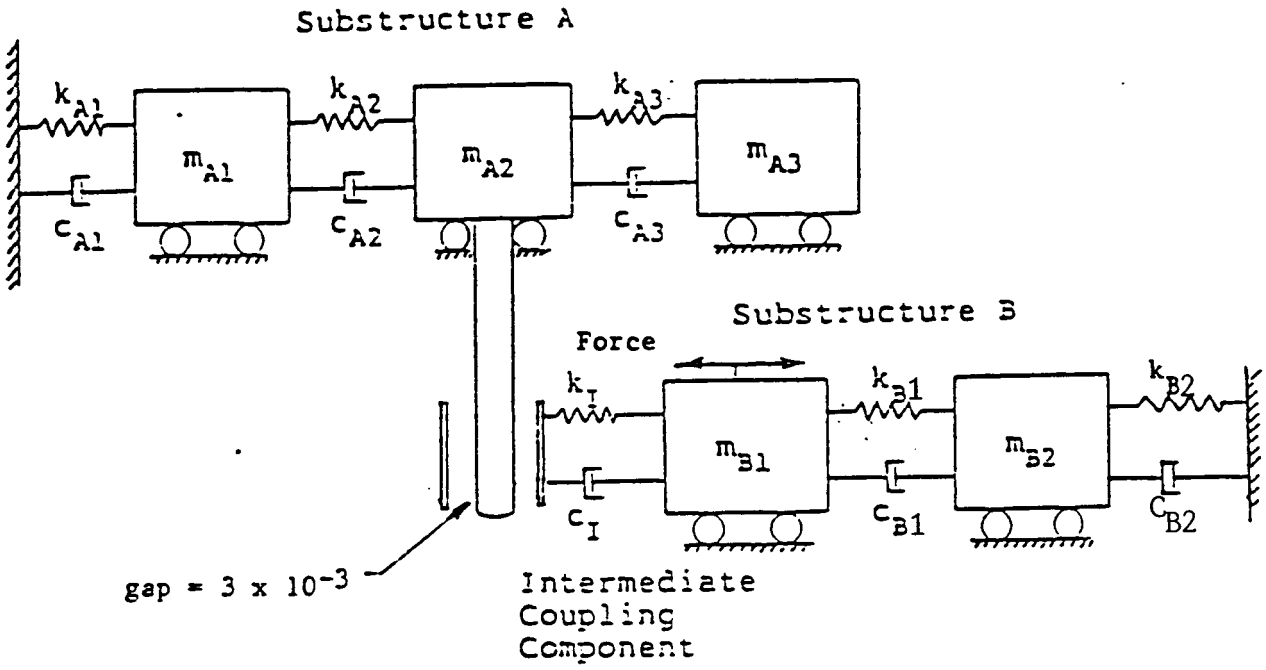

m_{A1}	= 6.25	K_{A1}	= 2 x 10^5	C_{A1}	= 10
m_{A2}	= 1	K_{A2}	= 6 x 10^5	C_{A2}	= 30
m_{A3}	= 1	K_{A3}	= 18 x 10^5	C_{A3}	= 90
m_{B1}	= 2	K_{B1}	= 2 x 10^5	C_{B1}	= 10
m_{B2}	= 4	K_{B2}	= 2 x 10^5	C_{B2}	= 10

$K_I = 2 \times 10^6$ $\qquad$ $C_I = 100$

Force = 20000 sin $\dot{\phi}t$

$\dot{\phi} = 550$

Figure A.1. The test model.